doi:10.1006/jmbi.2000.3555 available online at http://www.idealibrary.com on IDEAL® J. Mol. Biol. (2000) 297, 49–65

JMB

Roles of the *cco*GHIS Gene Products in the Biogenesis of the cbb_3-Type Cytochrome *c* Oxidase

Hans-Georg Koch[1], Christine Winterstein[1], A. Sami Saribas[1] James O. Alben[2] and Fevzi Daldal[1]*

[1]*Department of Biology, Plant Science Institute, University of Pennsylvania, Philadelphia, PA 19104-6018, USA*

[2]*Department of Medical Biochemistry, The Ohio State University, Columbus, OH 43210, USA*

**Corresponding author*

In many bacteria the *cco*GHIS cluster, located immediately downstream of the structural genes (*cco*NOQP) of cytochrome cbb_3 oxidase, is required for the biogenesis of this enzyme. Genetic analysis of *cco*GHIS in *Rhodobacter capsulatus* demonstrated that *cco*G, *cco*H, *cco*I and *cco*S are expressed independently of each other, and do not form a simple operon. Absence of CcoG, which has putative (4Fe-4S) cluster binding motifs, does not significantly affect cytochrome cbb_3 oxidase activity. However, CcoH and CcoI are required for normal steady-state amounts of the enzyme. CcoI is highly homologous to ATP-dependent metal ion transporters, and appears to be involved in the acquisition of copper for cytochrome cbb_3 oxidase, since a CcoI-minus phenotype could be mimicked by copper ion starvation of a wild-type strain. Remarkably, the small protein CcoS, with a putative single transmembrane span, is essential for the incorporation of the redox-active prosthetic groups (heme *b*, heme b_3 and Cu) into the cytochrome cbb_3 oxidase. Thus, the *cco*GHIS products are involved in several steps during the maturation of the cytochrome cbb_3 oxidase.

Keywords: biogenesis of membrane protein complexes; copper homeostasis; CPx-type ATPase; *c*-type cytochromes; photosynthesis and respiration

Introduction

The Gram-negative facultative photosynthetic bacterium *Rhodobacter capsulatus* is a versatile organism able to grow under a wide variety of conditions, and has a highly branched energy transducing electron transfer chain (Zannoni, 1995). Under photosynthetic (Ps) growth conditions, it uses a cyclic electron transfer pathway between the photochemical reaction center (RC) and the ubihydroquinone: cytochrome (cyt) *c* oxidoreductase (cyt bc_1 complex). On the other hand, its respiratory electron transfer pathways are branched after the quinone pool (Q_{pool}), and it contains a cyt *c* oxidase (C_{ox}) and a ubihydroquinone oxidase (Q_{ox}) as terminal oxidases (La Monica & Marrs, 1976; Zannoni *et al.*, 1976).

The *R. capsulatus* C_{ox} is of cbb_3-type (Gray *et al.*, 1994), and is encoded by the *cco*NOQP operon (Koch *et al.*, 1998; Thöny-Meyer *et al.*, 1994). A similar operon, called *fix*NOQP, has been described in various species including *Rhizobium meliloti* (Kahn *et al.*, 1989), *Bradyrhizobium japonicum* (Preisig *et al.*, 1993), *Rhodobacter sphaeroides* (Garcia-Horsman *et al.*, 1994a) and *Paracoccus denitrificans* (de Gier *et al.*, 1996). The cyt cbb_3 oxidases are members of the heme-Cu oxidase superfamily (Garcia-Horsman *et al.*, 1994b). Unlike the better characterized aa_3-type cyt *c* oxidases, these lack a Cu_A center and two of their subunits are membrane-bound monoheme (CcoO/FixO) and diheme

Present addresses: H.-G. Koch, Institut für Biochemie und Molekularbiologie, Albert-Ludwigs Universität-Freiburg, Hermann-Herder Strasse 7, 79104 Freiburg, Germany; S. Saribas, Department of Anesthesiology, University of Michigan Medical School, Ann Arbor, MI 48105, USA.

H.-G.K. and C.W. contributed equally to this work.

Abbreviations used: cyt, cytochrome; C_{ox}, cyt *c* oxidase; FTIR, Fourrier-transformed infrared; Med A, minimal medium A; MPYE, enriched medium; NADI, staining for cyt *c* oxidase activity; ONPG, *o*-nitrophenyl-β-D-galactopyranoside; Ps, photosynthetic; Q_{pool}, quinone pool; RC, reaction center; E_{m7}, redox midpoint potential; TMPD, 2,3,5,6-tetramethyl-1,4-phenylenediamine; Q_{ox}, ubihydroquinone oxidase.

E-mail address of the corresponding author: fdaldal@sas.upenn.edu

0022-2836/00/010049–17 $35.00/0

(CcoP/FixP) *c*-type cytochromes. The deduced amino acid sequences of their subunit I (CcoN/FixN) are highly homologous to those of the subunit I of the *aa*$_3$-type cyt *c* oxidases (Garcia-Horsman *et al*., 1994b). Both types of oxidase contain a binuclear center, composed of a copper atom (Cu$_B$) and a high-spin heme molecule (heme *a*$_3$ or *b*$_3$), where the reduction of oxygen to water takes place. They also contain a low-spin heme group (heme *a* or *b*) which channels electrons to the Fe-Cu binuclear center.

In most organisms characterized so far, *cco(fix)*-NOQP are located upstream of the *cco(fix)*GHIS cluster (Kahn *et al*., 1989; Preisig *et al*., 1996; de Gier *et al*., 1996; Koch *et al*., 1998). Early studies using *R. meliloti* have revealed that these gene clusters are co-regulated, and that mutations in either one resulted in a symbiotic nitrogen fixation (Fix$^-$) defect (for a review, see Batut & Boistard 1994). In *B. japonicum*, Preisig *et al*. (1996) demonstrated that deleting *cco(fix)*GHI decreased C$_{ox}$ activity in cells grown under oxygen deprivation conditions, and led to a Fix$^-$ phenotype like the *cco(fix)*NOQP mutants. On the other hand, in *R. sphaeroides* RdxB$^-$ (*rdx*BHIS is identical with *cco/fix*GHIS in this species), mutants are not impaired in cyt *cbb*$_3$ oxidase activity. However, they increase photosynthetic gene expression and alter carotenoid contents under aerobic growth conditions (O'Gara & Kaplan, 1997), as apparently does a CcoQ$^-$ mutant, which also has an active cyt *cbb*$_3$ oxidase (Oh & Kaplan, 1999). Genetic organization of the *cco*GHIS cluster is unknown, and the available deletions often encompass several of these genes, leaving undefined those required for the presence of an active cyt *cbb*$_3$ oxidase.

Earlier, Kahn *et al*. (1989) proposed that Cco(Fix)G may be involved in a redox process, possibly coupled to Cco(Fix)I working as a cation pump. More recently, an oxidoreductase role was put forward for CcoG (Preisig *et al*., 1996) based on its two cysteine-rich motifs resembling those encountered in the (4Fe-4S) cluster containing ferredoxin molecules (for a review, see Beinert *et al*., 1997). The deduced amino acid sequence of CcoG is also highly homologous to the RdxA of *R. sphaeroides*, which was suggested to catalyze some unknown redox process (Neidle & Kaplan, 1992). On the other hand, CcoI is thought to be important for Cu-homeostasis (Preisig *et al*., 1996) because of its significant sequence homology to CPx-type ATPases, like CopA and CopB, known to transport Cu in *Enterococcus hirae* (Odermatt *et al*., 1993; Solioz & Odermatt, 1995). CPx-type ATPases are crucial for homeostasis of potentially hazardous heavy metal ions in biological fluids, and are evolutionary well conserved (Solioz & Vulpe, 1996). Finally, CcoH and CcoS contain no characteristic motif, and have no homology to proteins of known function, leaving their roles completely unknown.

Using a genetic screen, we have recently identified four different classes of mutations affecting cyt *cbb*$_3$ oxidase activity in *R. capsulatus*, and characterized one of them in detail (Koch *et al*., 1998). Here, we show that two of the remaining classes contain mutations located within the *cco*GHIS cluster despite their different phenotypes. In addition, using appropriate polar and non-polar mutations and reporter gene fusions, we establish that *cco*G, *cco*H, *cco*I and *cco*S can be expressed independently from each other, implying that *cco*GHIS does not form a simple operon. Finally, we demonstrate that CcoH, CcoI and CcoS are involved in distinct maturation steps during the biogenesis of the cyt *cbb*$_3$ oxidase, possibly including acquisition of Cu, steady-state stability of the enzyme in the membrane and insertion of its *b*-type hemes and Cu cofactors.

Results

R. capsulatus C_{ox}^- mutants located in *cco*GHIS

We had previously described that some of the *R. capsulatus* C_{ox}^- (NADI$^-$) mutants like BK5 contained full amounts, while others like SS33 harbored only trace amounts, of the subunits of cyt *cbb*$_3$ oxidase in chromatophore membranes (Koch *et al*., 1998). Here, those mutants which are not complemented by the structural genes (*cco*NOQP) of cyt *cbb*$_3$ oxidase were further studied. Complementation of SS33 to a NADI$^+$ phenotype with a genomic library, constructed using *Bam*HI generated chromosomal DNA fragments, yielded plasmid pS33, which did not complement BK5. Similarly, complementation of BK5 with a genomic library constructed using *Hin*dIII generated chromosomal DNA fragments, yielded pBK1, which could not complement SS33. Mapping and sequence analyses of pS33 and pBK1 indicated that they contained partially overlapping DNA fragments carrying portions of *cco*GHIS (part of *cco*G, entire *cco*H and *cco*I and part of *cco*S in pS33, and part of *cco*I and entire *cco*S in pBK1) located immediately downstream of *cco*NOQP (Figure 1). Thus, both SS33 and BK5 contained mutations located in *cco*GHIS, despite their different phenotypes. In addition, it was deduced that the mutation in BK5 must be in *cco*S, which was the only intact gene in pBK1. Indeed, sequence analysis of an appropriate fragment after PCR amplification using BK5 chromosomal DNA as a template established that this mutant had a G to A nucleotide substitution at base-pair position 71 of *cco*S, resulting in a premature stop codon (TGG to TAG).

Mutational inactivation of the entire *cco*GHIS cluster

Considering that *cco*GHIS deletions abolished the presence of an active cyt *cbb*$_3$ oxidase in *R. meliloti* (Batut & Boistard, 1994) and *B. japonicum* (Preisig *et al*., 1996), it was analyzed whether this was also the case in *R. capsulatus*. The *R. capsulatus*

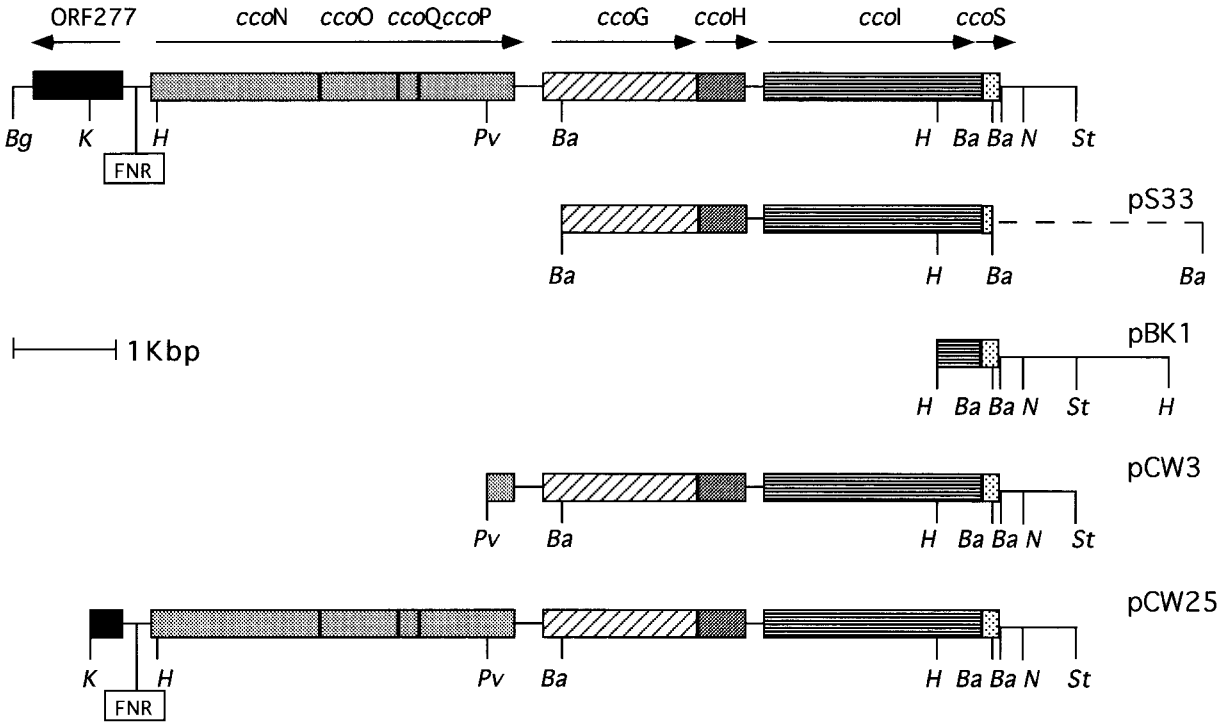

Figure 1. The *cco*NOQP and *cco*GHIS clusters of *R. capsulatus*. Plasmids carrying various portions of these genes are shown, and the restriction endonucleases *Bam*HI (*Ba*), *Bgl*II (*Bg*), *Hin*dIII (*H*), *Kpn*I (*K*), *Nru*I (*N*), *Pvu*II (*Pv*) and *Stu*I (*St*) cleavage sites are indicated. Arrows correspond to the transcription directions of the genes, and the putative FnrL binding site in front of *cco*NOQP is boxed.

mutant CW1 containing a complete deletion-insertion allele of *cco*GHIS (Δ(*cco*GHIS::*spe*)) (Figure 2) was NADI$^-$ and its membranes lacked all subunits of cyt *cbb*$_3$ oxidase (Figure 3). Thus, deletion of *cco*GHIS also led to the absence of the cyt *cbb*$_3$ oxidase in *R. capsulatus*. As expected, CW1 was not complemented to NADI$^+$ by plasmid pOX15 carrying *cco*NOQP, but was readily complemented by either pCW3 or PCW25, which contained either only *cco*GHIS, or both *cco*NOQP and *cco*GHIS clusters, respectively (Figure 1). Both strains pCW3/CW1 and pCW25/CW1 had C_{ox} activity (Table 1). It was noted that the respiratory growth of CW1 was slower both in enriched MPYE or minimal Med A media than a C_{ox}^- mutant such as GK32 (Δ(*cco*NO::kan)) (Koch *et al.*, 1998). The poor respiratory growth phenotype of CW1 was complemented only by pCW25 (*cco*NOQP-*cco*GHIS), and not by pCW3 (*cco*GHIS), indicating that a DNA fragment carrying both of these clusters was necessary for its full complementation (see also Discussion).

Polar and non-polar *cco*G, *cco*H, *cco*I and *cco*S mutations

In *R. capsulatus* *cco*G, *cco*H, *cco*I and *cco*S are located very close to each other, only separated by 25, 150 and 17 bp, respectively. Thus, polar and non-polar mutations located in each of these genes were sought to define the transcriptional organization of *cco*GHIS. As described in Materials and Methods, non-polar *cco*G, *cco*H and *cco*I deletion alleles were constructed yielding pCW15 (Δ*cco*G), pCW17 (Δ*cco*H), pCW9 (Δ*cco*I), respectively. In addition, plasmid pS33 (Figure 1) provided a deletion allele of *cco*S, truncated at its 3′ end. These plasmids were also used to obtain polar deletion-insertion alleles of *cco*G (Δ(*cco*G::*spe*) on pCW16), *cco*I (Δ(*cco*I::*spe*) on pCW8) and *cco*S (Δ(*cco*S::*kan*) on pBK1F) and an insertion allele of *cco*H ((*cco*H::*kan*) on pCW18). These polar mutations were introduced into the chromosome of the wild-type *R. capsulatus* strain MT1131, as described in Materials and Methods, yielding null CcoG$^-$ (CW5), CcoH$^-$ (CW6), CcoI$^-$ (CW2) and CcoS$^-$ (BK6) mutants (Figure 2). Of these, CW6, CW2 and BK6 were NADI$^-$, while CW5 was NADI^{slow} on MPYE and NADI$^+$ on MedA plates. Membranes from CW6 (CcoH$^-$) and CW2 (CcoI$^-$), like those from CW1 (Cco(GHIS)$^-$) or GK32 (C_{ox}^-), catalyzed no TMPD oxidase reaction (Table 1), and contained no, or highly decreased, amounts of the cyt *cbb*$_3$ oxidase subunits (Figure 3). On the other hand, BK6 (CcoS$^-$) and CW5 (CcoG$^-$) harbored all subunits of the cyt *cbb*$_3$ oxidase at quasi-wild-type levels (Figure 3), but only the CcoG$^-$ mutant (CW5) had significant amounts of C_{ox} activity, while the CcoS$^-$ mutant (BK5) produced an inactive enzyme (Table 1).

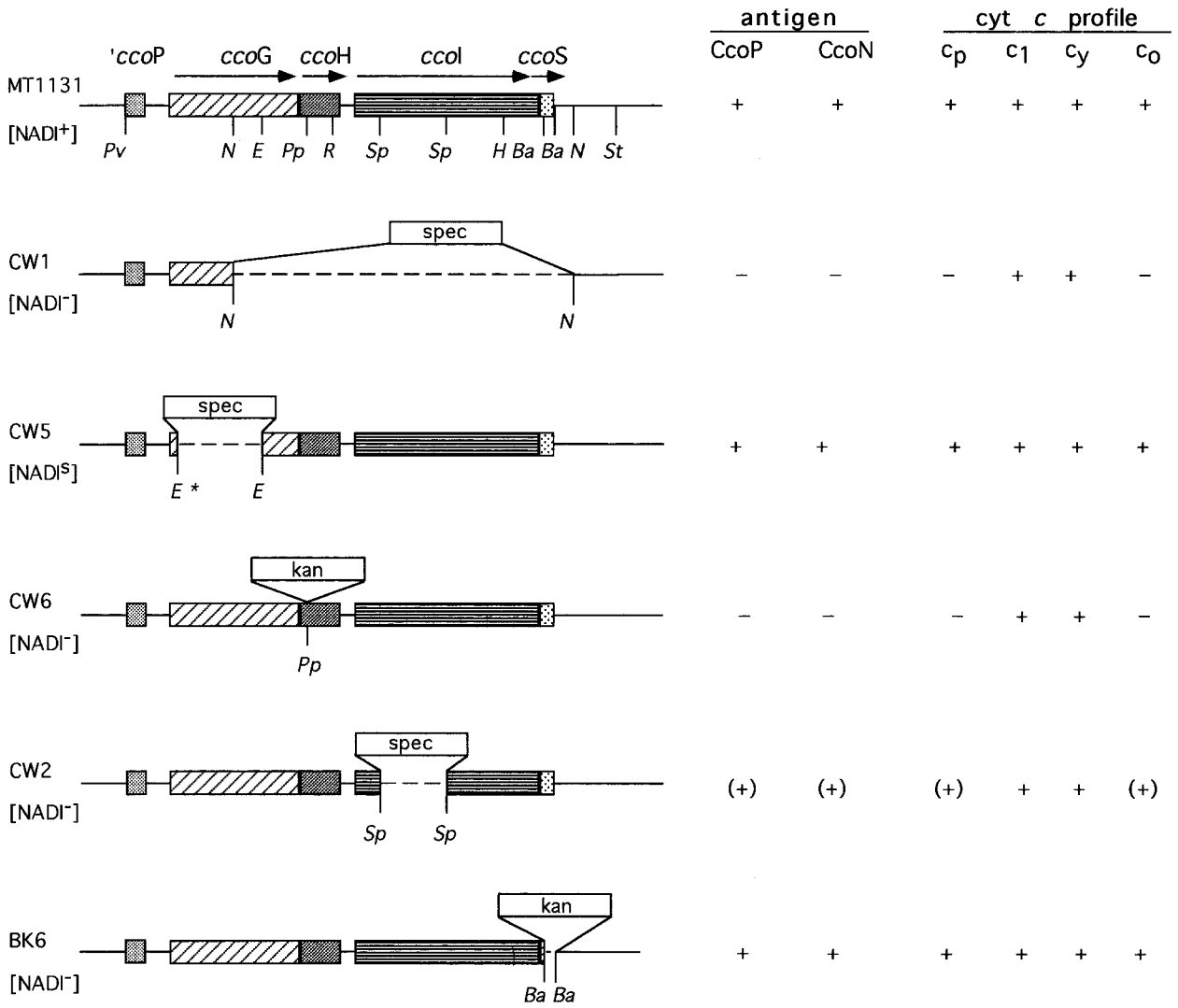

Figure 2. Chromosomal locations of various *cco*GHIS mutations, their NADI phenotypes and cyt *cbb*$_3$ oxidase subunit compositions. *Eco*72 I (*E*), *Ppu*MI (*Pp*), *Rsr*II and *Sp*hI (*Sp*) refer the restriction enzymes cleavage sites shown in addition to those already presented in Figure 1, and E* indicates the silent site created by site-directed mutagenesis, as described in Materials and Methods. For NADI phenotype +, – or s indicate positive, negative or slow, respectively, and spec and kan correspond to spectinomycin and kanamycin resistance conferring genes. The subunits of the cyt *cbb*$_3$ oxidase were revealed by using either polyclonal antibodies against the subunits I (CcoN) or II (CcoP) of *R. capsulatus* enzyme, or by TMBZ staining for the *c*-type cytochrome subunits II (CcoP) and III (CcoO). The cyt c_1 and c_y correspond to the cyt c_1 subunit of the cyt bc_1 complex, and the membrane-attached electron carrier cyt c_y, respectively. The symbols +, (+) or – indicate the presence, reduction or absence of the cytochromes or subunits CcoP or CcoN in chromatophore membranes of the corresponding strains.

Transcriptional organization of *cco*GHIS

The ability of various plasmids with polar and non-polar *cco*G, *cco*H, *cco*I and *cco*S mutations to complement the chromosomal null CcoG$^-$, CcoH$^-$, CcoI$^-$ and CcoS$^-$ mutants for NADI$^+$ phenotype on MPYE medium was determined (Table 2). The data revealed that identical complementation patterns were seen with pCW15 (Δ(*cco*G)) and pCW16 (Δ(*cco*G::*spe*)), with pCW17 (Δ(*cco*H)) and pCW18 (Δ(*cco*H::*kan*)), and with pCW9 (Δ(*cco*I)) and pCW8 (Δ(*cco*I::*spe*)) pairs. This suggested that the polar mutations in CW5, CW6 and CW2 did not abolish completely expression of the downstream genes, inferring that *cco*G, *cco*H and *cco*I could be expressed independently from each other. Similarly, crosses using pS33, pBK1 and pBK1F indicated that *cco*S could be expressed independently from *cco*GHI. The crosses also showed that SS33 was complemented with plasmids carrying non-polar or polar mutations in either *cco*G (pCW15 or pCW16) or *cco*H (pCW17 or pCW18), but not in *cco*I (pCW9 and pCW8). Thus, SS33 contained a defective *cco*I, consistent with its C_{ox}^-/NADI$^-$ phenotype.

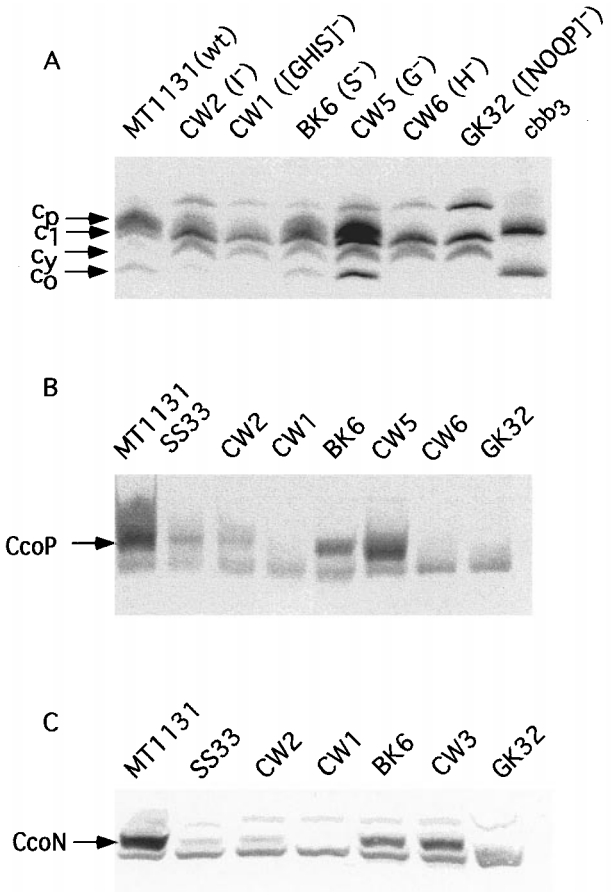

Figure 3. Presence of cytochrome cbb_3 subunits in various *cco*GHIS mutants. (a) TMBZ/SDS-PAGE analyses of the *c*-type cytochromes detected in chromatophore membranes of various mutants grown in MPYE enriched medium. Total membrane proteins (180 μg) for the strains or 2 μg of purified cyt cbb_3 oxidase were loaded per lane. The cytochromes c_P and c_o correspond to the subunits II and III of the cyt cbb_3 oxidase, and c_1 and c_y correspond to the cyt c_1 subunit of the cyt bc_1 complex and the membrane-attached electron carrier cyt c_y, respectively. The mutations carried by each strain are shown between parentheses, and wt indicates a wild-type background. (b) and (c) Immunoblot analyses of appropriate *cco*GHIS mutants using polyclonal antibodies against the subunit II (CcoP) and subunit I (CcoN) of *R. capsulatus* cyt cbb_3 oxidase, respectively. For the immunoblots, 10 μg of membrane proteins per lane were used. Following SDS-PAGE, proteins were transferred onto an Immobilon-P membrane, and detected using horseradish peroxidase-conjugated anti-rabbit secondary antibodies and 3,3′-diaminobenzidine as a substrate in the presence of $NiCl_2$. The subunits CcoN and CcoP are indicated with arrows, and the additional bands correspond to non-specific reactions with the antibodies used. SS33 carries a mutation in *cco*I, BK6 and CW3 are allelic for *cco*S, and the other strains are as indicated in (a).

*cco*G::*lac*Z, *cco*H::*lac*Z, *cco*I::*lac*Z and *cco*S::*lac*Z translational fusions

To firmly establish that *cco*G, *cco*H, *cco*I and *cco*S could be expressed independently from each other, appropriate DNA fragments (Figure 4(a)) were cloned in front of a promoter-less *lac*Z on plasmid pXCA601 as described in Materials and Methods. The *cco*G::*lac*Z, *cco*H::*lac*Z, *cco*I::*lac*Z and *cco*S::*lac*Z translational fusions thus obtained were introduced into MT1131, and the β-galactosidase activities in these strains grown under semi-aerobic conditions in enriched MPYE medium were determined (Figure 4(b)). The data demonstrated that *cco*G, *cco*H, *cco*I and *cco*S could be transcribed independently from each other. Moreover, expression of the *cco*GHIS genes were of different levels, with those of *cco*H and *cco*S being about four- to eight-fold higher than those of *cco*G and *cco*I. The extent to which the expression of each gene also contributed to the overall expression of the downstream genes was not determined.

CcoG is not a transcriptional regulator of *cco*NOQP operon

A previously constructed *cco*N::*lac*Z translational fusion (pXG2) (Koch *et al.*, 1998) was used to determine whether or not CcoG affects the transcription of *cco*NOQP. In addition, the effect of FnrL, known to regulate the expression of *R. sphaeroides cco*NOQP (Mouncey & Kaplan, 1998), was also tested using the *R. capsulatus* Fnr$^-$ mutant RGK295 (Zeilstra-Ryalls *et al.*, 1997). The β-galactosidase activities expressed in a wild-type strain and in the CcoG$^-$ and FnrL$^-$ mutants were determined under various growth conditions, and in both MPYE-enriched (Figure 5) and MedA-minimal media (not shown). The data revealed that comparable amounts of β-galactosidase activities were found in all three strains under any given growth condition. Thus, neither *cco*G nor *fnr* significantly affects the expression of *R. capsulatus cco*NOQP. Interestingly, under semi-aerobic growth conditions, expression of the *cco*N::*lac*Z fusion was about twofold higher than that seen under photosynthetic or aerobic growth conditions (Figure 5), and there was also about a twofold increase in minimal *versus* MPYE media (data not shown).

CcoH and CcoI are required for normal steady-state amounts of *R. capsulatus* cyt *cbb*$_3$ oxidase

Introduction of the plasmid pXG2 into the CcoH$^-$ (CW6) and CcoI$^-$ (CW2) mutants showed that neither *cco*H nor *cco*I drastically affected the expression of *cco*N::*lac*Z fusion (data not shown). Yet, in these mutants, the steady-state amounts of the cyt cbb_3 oxidase subunits were extremely low (Figure 3), although the amounts of other cytochromes, such as for example those of the cyt bc_1 complex, were unchanged (Figure 3, and data not

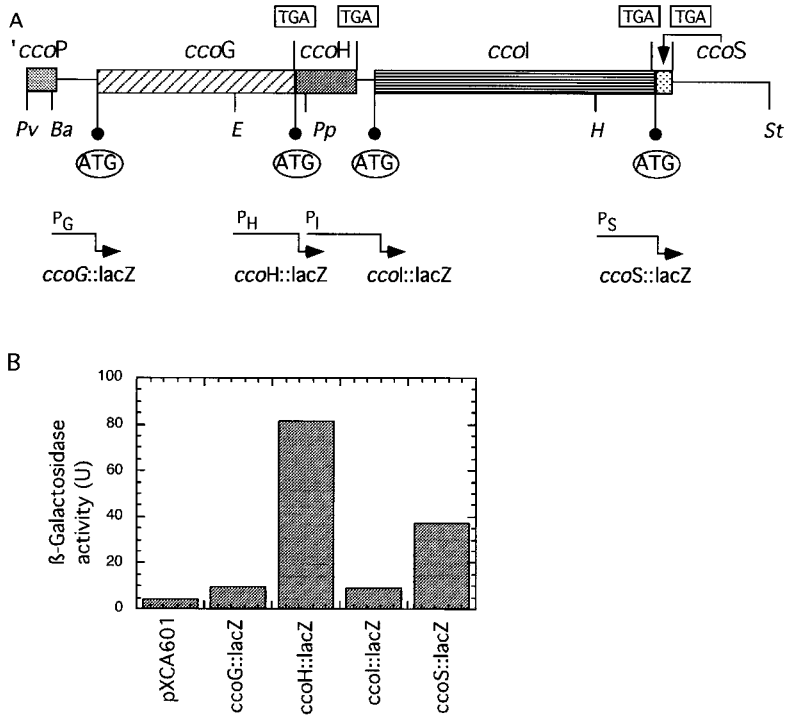

Figure 4. Various *cco*GHIS::*lac*Z translational fusions. (a) On the *cco*GHIS region of *R. capsulatus* the locations of the putative promoters P_G, P_H, P_I and P_S and the initiation (ATG) and termination (TGA) codons of *cco*G, *cco*H, *cco*I and *cco*S are indicated, and the restriction enzyme cleavage sites are as described in the legend to previous Figures. The DNA fragments used to construct the *cco*G::*lac*Z, *cco*H::*lac*Z, *cco*I::*lac*Z and *cco*S::*lac*Z translational fusions carrying the indicated promoter activities are shown by arrows. (b) The bar graph indicates the β-galactosidase activities in units (1 unit = 1 nmol of ONPG hydrolyzed per ml per minute per mg of protein) measured in cell extracts of the different derivatives of strain MT1131 harboring the appropriate fusions and grown under semi-aerobic conditions in MPYE-enriched medium. pXCA601 refers to the control plasmid containing the promoter-less *lac*Z used to construct these fusions.

shown). These findings therefore indicated that *cco*H and *cco*I affected cyt cbb$_3$ oxidase activity at a post-translational level. CcoH has no homology to any protein of known function, but CcoI is highly homologous to CPx-type ATP-dependent metal ion transporters (Solioz & Vulpe, 1996), containing at their amino terminal a CxyC motif thought to be important for metal binding. Whether this motif is also required for the function of *R. capsulatus* CcoI was tested by substituting its second Cys residue (Cys12 in *R. capsulatus* CcoI) with a serine residue by site-directed mutagenesis. Indeed, the mutant pCW21/CW2 thus obtained was NADI^{slow} and contained lower amounts of cyt *cbb*$_3$ oxidase sub-

Table 1. Cyt *cbb*$_3$ activity in various CcoGHIS mutants

Strains	Genotype	O_2 consumption[a]	% of wild-type activity
MT1131	wild-type (wt)	38	100
GK32[b]	(Δ*cco*NO::*kan*)	0	0
CW1	(Δ*cco*GHIS::*spe*)	0	0
pCW3/CW1	*cco*GHIS in Δ(*cco*GHIS::*spe*)	30	80
pOX15[b]/MT1131	*cco*NOQP	184	490
pCW25/CW1	*cco*NOQP+ccoGHIS in Δ(*cco*GHIS::*spe*)	145	380
CW5	Δ(*cco*G::*spe*)	33	90
CW6	*cco*H::*kan*	0	0
CW2	Δ(*cco*I::spe)	0	0
BK6	Δ(*cco*S::kan)	0	0

Chromatophore membranes of the wild-type strain MT1131 and its *cco*GHIS-minus derivatives grown semi-aerobically in MPYE-enriched medium were assayed for TMPD/ascorbate oxidase activity as described in Materials and Methods.

[a] The μmol of O_2/h/mg of protein.

[b] From Koch *et al.* (1998).

Table 2. NADI phenotypes of various *R. capsulatus* merodiploids obtained by complementation of chromosomal null *cco*GHIS mutants with plasmids carrying either polar or non-polar mutations in *cco*G, *cco*H, *cco*I and *cco*S

	WT		G^-		H^-		I^-		S^-		S^+
Plasmids and their phenotypes	pCW25	pCW3	pCW15	pCW16	pCW17	pCW18	pCW9	pCW8	pS33	pBK1F	pBK1
	N^+ G^+	G^+	G^-	G::*spe*	G^+	G^+	G^+	G^+	G′	I′	I′
	O^+ H^+	H^+	H^+	H^+	H^-	H::*kan*	H^+	H^+	H^+	S::*kan*	S^+
	Q^+ I^+	I^+	I^+	I^+	I^+	I^+	I^-	I::*spe*	I^+		
	P^+ S^+	S^+	S^+	S^+	S^+	S^+	S^+	S^+	S^-		
Recipients and their genotypes											
MT1131 (wild-type)	+	+[a]	nd	nd	nd	nd	nd	nd	nd	nd	nd
CW1 Δ(*ccoGHIS::spe)*	+	+	s	s	−	−	−	−	−	−	−
CW5 Δ(*ccoG::spe)*	+	+	s[a]	s	+	+	+	+	s	nd	nd
CW6 *ccoH::kan*	+	+	+	+	−	−	+	+	+	nd	nd
CW2 Δ(*ccoI::spe)*	+	+	+	+	+	+	−	−	+	nd	nd
BK6 Δ(*ccoS::kan)*	+	+	+	+	+	+	+	+	−	−	+
SS33 (*ccoI33)*	+	+	+	+	+	+	−	−	+	nd	−

[a] +, − and s indicate $NADI^+$, $NADI^-$ and $NADI^{slow}$ phenotypes, nd corresponds to not determined and ′ indicates incomplete genes.

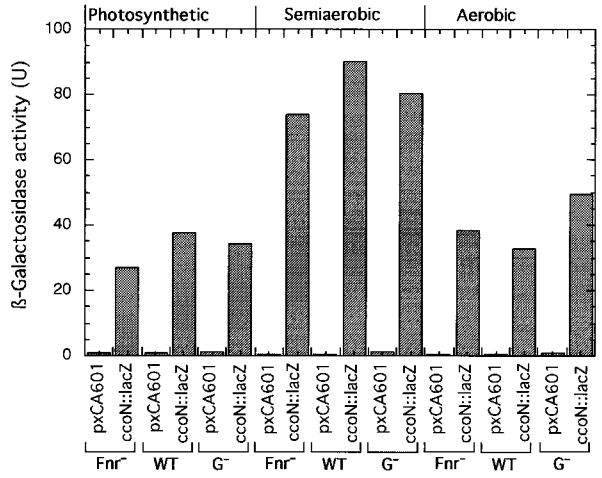

Figure 5. Effects of *cco*G and *fnr*L mutations on the expression of the *cco*NOQP encoding the cyt *cbb*$_3$ oxidase of *R. capsulatus*. The bar graph indicates the β-galactosidase activities (in units, as described in the legend to Figure 4) found in crude extracts of a wild-type strain (MT1131) and the CcoG$^-$ (CW5) and Fnr$^-$ (RGK295) mutants harboring the *cco*N::*lac*Z fusion pXG2 or the control plasmid pXCA601 grown under photosynthetic, semi-aerobic and aerobic conditions in MPYE-enriched medium.

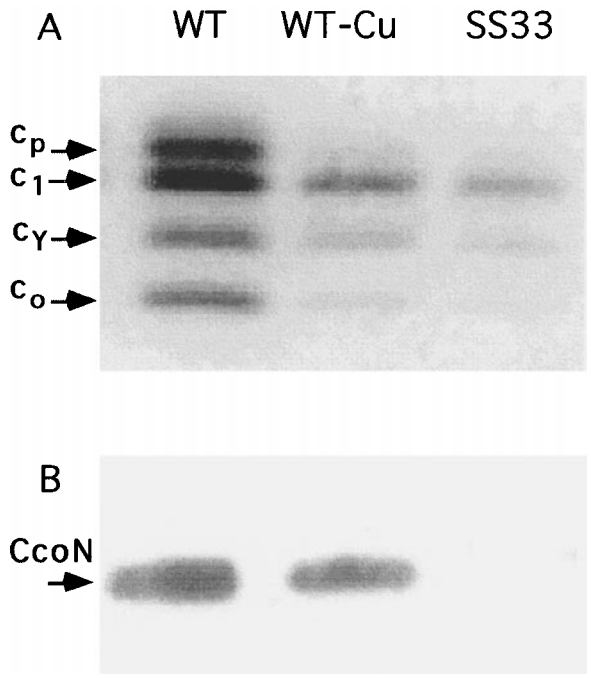

Figure 6. Effect of copper-depletion on the steady-state amount of *R. capsulatus* cyt *cbb*$_3$ oxidase. Steady-state amounts of the cyt *cbb*$_3$ oxidase subunits in the wild-type strain MT1131 (WT) and the CcoI$^-$ mutant SS33 (SS33) grown in Med A minimal medium under semi-aerobic conditions were compared with those found in the same wild-type strain grown in Cu-depleted Med A (WT-Cu) minimal medium under the same growth conditions, as described in Materials and Methods. Total membrane proteins (100 and 10 µg) per lane were loaded for TMBZ/SDS-PAGE analysis of the *c*-type cytochromes revealing the subunits II and III (a), and immunoblot detection (b) of the subunit I of *R. capsulatus* cyt *cbb*$_3$ oxidase, respectively. All other experimental conditions were as in Figure 3.

units (data not shown), indicating that this motif was also important for the function of *R. capsulatus* CcoI.

Copper is the only other catalytic metal ion in the cyt *cbb*$_3$ oxidases besides the heme iron, and it was therefore analyzed as to whether CcoI is involved in its acquisition. We found that while addition of exogenous Cu does not phenotypically complement a CcoI$^-$ mutant (data not shown), its depletion severely affects the C_{ox} activity in a wild-type strain. TMPD/ascorbate-induced oxygen uptake activity was measured using whole cells of MT1131 grown in Med A (containing 1570 nM of Cu), Cu-depleted Med A (containing <315 nM of Cu) and Cu-depleted Med A media supplemented with various concentrations of $CuSO_4$. In Med A medium the oxygen uptake activity exhibited by MT1131 was about 11 (±1.4) µmol O_2 per hour per mg of protein; in Cu-depleted Med A this value decreased to about 0.7 (±0.15) µmol O_2 per hour per mg of protein. This activity could be restored almost completely by supplementing the Cu-depleted Med A medium with 1.6 to 4.8 µM of $CuSO_4$, suggesting that it was due to Cu depletion. A similar effect was also seen when membranes, instead of whole cells, were used for oxygen uptake measurements. TMBZ/SDS-PAGE and immunoblot analyses of membranes derived from the Cu-depleted cells revealed that the amounts of the CcoP (cyt c_p), CcoO (cyt c_o) and CcoN subunits of cyt *cbb*$_3$ oxidase were reduced, while other cytochromes, such as cyt c_1 and cyt c_y were less affected (Figure 6). The similarity of this phenotype induced in a wild-type strain by Cu-depletion to that of a CcoI$^-$ (CW2) or a CcoH$^-$ (CW6) mutant, in combination with the striking sequence homology between CcoI and heavy-metal ion transporting CPx-type ATPases, suggested that CcoI is probably involved in the acquisition of Cu for the cyt *cbb*$_3$ oxidase. However, CcoH$^-$ and CcoI$^-$ mutants are neither resistant nor hypersensitive to exogenous copper ions (data not shown), as could have been expected with a generic transport defect, suggesting the presence of additional Cu transport systems.

CcoS is required for the presence of heme *b*, heme *b*$_3$ and Cu$_B$ cofactors of the CcoN subunit of cyt *cbb*$_3$ oxidase

Chromatophore membranes of a CcoS$^-$ mutant such as BK6 contain all three subunits of the cyt *cbb*$_3$ oxidase at quasi-wild-type amounts, despite the lack of any enzymatic activity (Figure 3 and Table 1). Moreover, in such a mutant the CcoO (cyt

c_o) and CcoP (cyt c_p) subunits contain their *c*-type cytochromes as they are readily stained by TMBZ (Figure 3). Thus, the presence of the cofactors of the subunit I (CcoN) of the cyt *cbb*$_3$ oxidase was examined to account for the lack of C_{ox} activity in this mutant.

Membranes of a wild-type *R. capsulatus* strain such as MT1131 contain several *b*-type cytochromes absorbing at a wavelength of around 560 nm. Of these, two have redox midpoint potential (E_{m7}) values of approximately 400 mV and 270 mV, and correspond to the low-spin cyt *b* of the cyt *cbb*$_3$ oxidase, and to a *b*-type cyt component associated with the Q_{ox}, respectively (La Monica & Marrs, 1976; Zannoni *et al.*, 1976). Dark, anaerobic titrations of chromatophore membranes of appropriate strains revealed that in the CcoS$^-$ mutant BK5, like in the C_{ox}^- mutant GK32 (Δ(*cco*NO::*kan*)), the cyt *b* component with an E_{m7} value of 400 mV was absent, while that with an E_{m7} value of 270 mV was still detectable (data not shown). Examination of appropriate optical difference spectra (approximately 350 mV minus 430 mV range) obtained during these titrations revealed the absence of a 560 nm cyt *b* component in BK5 (CcoS$^-$) and GK32 (C_{ox}^-) which was visible in the wild-type strain MT1131 and the cyt *cbb*$_3$ oxidase overproducer mutant M6G (Figure 7(a)). Thus, in the absence of CcoS the low-spin cyt *b* cofactor of cyt *cbb*$_3$ oxidase was absent despite the presence of a full complement of the subunit I apoprotein.

Next using FTIR spectroscopy, which monitors the stretching frequencies of CO as a probe of its environment (Alben, 1993; Fiamingo & Alben, 1985), the CcoS$^-$ mutant was examined for the presence of cyt b_3-Cu_B binuclear center of the cyt *cbb*$_3$ oxidase. Combined with photolysis at low temperature, FTIR spectroscopy readily reveals the formation of both CO-Fe and CO-Cu adducts in heme-copper oxidases, and reports on the presence or absence of the heme Fe of cyt b_3 and Cu_B atom at the binuclear center. Membranes from the *R. capsulatus* Q_{ox}^- mutant M6G, which produces copious amounts of cyt *cbb*$_3$ oxidase, showed a Fe-CO band at 1954 cm^{-1}, with a shoulder at 1969 cm^{-1}, visible as a sharp trough in the difference spectrum (Figure 7(b), lower trace). Upon photolysis, CO absorbs at a higher frequency yielding a band at 2063 cm^{-1}, indicative of a Cu-CO complex (Fiamingo *et al.*, 1982). The Fe-CO band at 1954 cm^{-1} and the Cu-CO band at 2063 cm^{-1} are identical with those observed with purified cyt *cbb*$_3$ oxidase from *R. capsulatus* (Fe-CO, 1954 cm^{-1} and Cu-CO, 2064 cm^{-1}, M. Lübben, personal communication) or *R. sphaeroides* (Fe-CO, 1952 cm^{-1} and Cu-CO, 2065 cm^{-1}) (Garcia-Horsman *et al.*, 1994a). Membranes of the C_{ox}^- mutant GK32 (Δ(*cco*NO::*kan*)) and the CcoS$^-$ mutant BK5 lacked both of these bands, but exhibited a Fe-CO band at 1971 cm^{-1}, also present as a shoulder in M6G. While the origin of the 1971 cm^{-1} band is unknown, the absence of the 1952 cm^{-1} and 2063 cm^{-1} bands in BK5 and GK32 clearly

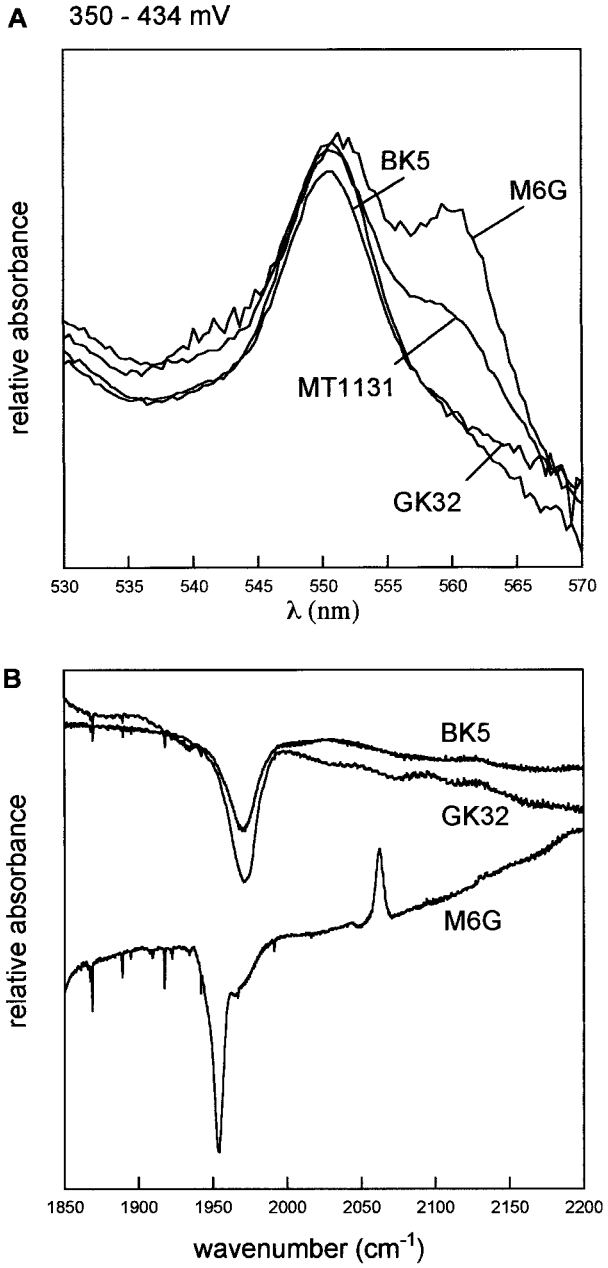

Figure 7. Absence of the redox-active cofactors of the cyt *cbb*$_3$ oxidase in a CcoS$^-$ mutant of *R. capsulatus*. (a) Reduced minus oxidized optical absorption difference spectra of *R. capsulatus* strains MT1131 (wild-type), M6G (C_{ox} overproducer, Q_{ox}^-), BK5 (CcoS$^-$) and GK32 (C_{ox}^-, Q_{ox}^+). The difference spectra shown were obtained by subtracting the spectra recorded at E_h values around 430 mV from those recorded at around 350 mV during the reductive titrations of the *b*-type cytochromes (monitored at 560 - 570 nm) present in chromatophore membranes of cells grown in MPYE enriched medium. (b) FTIR difference spectra (reduced anaerobic CO dark spectrum minus light spectrum after photolysis) are shown for BK5 (CcoS$^-$), M6G (C_{ox} overproducer, Q_{ox}^-) and GK32 (C_{ox}^-, Q_{ox}^+) in the range of 1850-2200 cm^{-1} at 20 K. The Fe-CO band at 1954 cm^{-1} and the Cu-CO band at 2063 cm^{-1}, which are missing in BK5 and GK32, correspond to the cyt *cbb*$_3$ oxidase of *R. capsulatus*. The origin of the band at 1971 cm^{-1} seen in GK32 and BK5, which is also present as a shoulder in M6G, is unknown.

indicated the absence of the cyt b_3-Cu_B binuclear center of the cyt *cbb*$_3$ oxidase. The overall data therefore indicated that CcoS is required for the presence of the cyt *b*, cyt b_3 and Cu_B cofactors of the cyt *cbb*$_3$ oxidase.

Discussion

Biogenesis of multisubunit metalloproteins requires accessory proteins involved in distinct post-translational modification steps, extending from translocation of the polypeptides across the membrane, to specific and kinetic insertion of their cofactors and stable assembly of the mature subunits (Merchant & Dreyfuss, 1998). In general, little is known about these processes. In the case of cyt *cbb*$_3$ oxidase, the requirement of *cco*GHIS for the biosynthesis of this enzyme was previously known in rhizobial species (Batut & Boistard 1994; Preisig *et al*., 1996). Here, analysis of *R. capsulatus* mutants lacking an active cyt *cbb*$_3$ oxidase due to mutations not located in *cco*NOQP extended the earlier findings to phototrophic species. Moreover, it also allowed us to ascribe specific roles to the *cco*GHIS products. The two distinct phenotypes of *R. capsulatus cco*GHIS mutants, like BK5 containing an assembled but inactive cyt *cbb*$_3$ oxidase and SS33 exhibiting extremely low amounts of this enzyme, suggested that the different products of *cco*GHIS might play different roles. Indeed, isolation of mutations separately abolishing *cco*H, *cco*I and *cco*S established that their products affect discrete maturation steps of cyt *cbb*$_3$ oxidase. These include the steady-state stability of the enzyme and the incorporation of its heme *b*, b_3 and Cu cofactors. The *cco*GHIS products appear to be remarkably specific to the cyt *cbb*$_3$ oxidases. At least in *B. japonicum* (Preisig *et al*., 1996), and possibly also in other organisms, absence of *cco*GHIS has no effect on the maturation of the closely reated cyt *aa*$_3$ oxidase.

An unexpected observation was the slow growth of the *cco*GHIS deletion mutant CW1. This growth defect does not originate from the absence of the C_{ox} activity since neither a C_{ox}^- mutant such as GK32 nor the single mutants CcoG$^-$, CcoH$^-$, CcoI$^-$ or CcoS$^-$ exhibit it. Its molecular basis has not been studied further, but a need of both *cco*GHIS and *cco*NOQP for its complementation, unlike the C_{ox}^- phenotype, suggests that it may arise from an imbalance between the products of these clusters.

In *R. melliloti* (Kahn *et al*., 1989) and *B. japonicum* (Preisig *et al*., 1996) homologs of *cco*GHIS have been proposed to form an operon, while in *R. sphaeroides*, the presence of a possible internal promoter within the cluster has been suggested (O'Gara & Kaplan, 1997). Complementation analyses and promoter localization studies reported here demonstrated that in *R. capsulatus cco*G, *cco*H, *cco*I and *cco*S have their own promoters of different strength, and can be expressed independently. However, whether or not under certain physiological conditions *cco*GHIS, or a part of it, is also expressed as a single transcript remains to be seen. In many bacteria, but not in *R. capsulatus,* a putative FNR-binding box is located upstream of both *cco*NOQP and *cco*GHIS (Koch *et al*., 1998) (Figure 1). Indeed, FnrL is a positive regulator of *cco*NOQP in *R. sphaeroides*, and is essential for photosynthetic and anaerobic dark growth in the presence of DMSO (Mouncey & Kaplan, 1998). In *R. capsulatus*, an FnrL$^-$ mutant is photosynthesis-proficient although it is unable to grow in anaerobic dark with DMSO (Zeilstra-Ryalls *et al*., 1997). The gene fusion data obtained here indicated no significant involvement of either FnrL or CcoG on the expression of *R. capsulatus cco*NOQP. It is noteworthy that most organisms characterized so far, except *R. capsulatus*, express multiple cyt *c* oxidases, with the cyt *cbb*$_3$ oxidase becoming selectively predominant under microaerobic conditions (Kahn *et al*., 1989; Preisig *et al*., 1996; Mouncey & Kaplan, 1998). In *R. capsulatus*, this enzyme is present under all oxygen tensions, and hence its regulation during respiratory growth has to be different.

In CcoG$^-$ mutant cyt *cbb*$_3$ oxidase exhibits substantial activity, indicating that it is not required for C_{ox} activity under the conditions tested here. Its absence in *R. capsulatus* also affects telluride reduction (to be reported elsewhere), as do its homologs RdxA (Neidle & Kaplan, 1992) and RdxB (O'Gara & Kaplan, 1997; Oh & Kaplan, 1999) in *R. sphaeroides*. Preisig *et al*. (1996) have proposed that CcoG might be involved in intracellular oxidation of Cu^+, which is probably the transported form of this metal (Hassett & Kosman, 1995; Lutsenko, *et al*., 1997; Odermatt *et al*., 1993), to its biologically utilized Cu^{2+} form (Figure 8). If this is the case, then the phenotype of *R. capsulatus* CcoG$^-$ mutants suggests either the presence of additional proteins catalyzing a similar reaction, or even the sufficiency of a non-enzymatic oxygen-dependent oxidation of Cu^+ to Cu^{2+} under some growth conditions. At low-oxygen tensions where the cyt *cbb*$_3$ oxidase becomes the main terminal oxidase, like in rhizobia during root nodule formation, it is conceivable that a non-enzymatic oxidation of Cu is insufficient to support intense energy requirements, hence there is a need for a specific CcoG-like oxidoreductase in performing this task. Rhizobial mutants lacking only CcoG may help to test the validity of this attractive hypothesis.

In the CcoH$^-$ or CcoI$^-$ mutants, extremely small amounts of cyt *cbb*$_3$ oxidase are present despite the wild-type levels of transcription of *cco*NOQP as evidenced by a *cco*N::*lac*Z fusion (data not shown). This suggests that in the absence of CcoH or CcoI cyt *cbb*$_3$ oxidase may be degraded rapidly (Figure 8). The predicted amino acid sequence of CcoH has no homology to proteins of known functions. Besides its two putative transmembrane helices, no structural motifs, and in particular no obvious cofactor or metal binding sites, are detectable in CcoH, leaving its role unknown. On the other hand, *R. capsulatus* CcoI with its eight

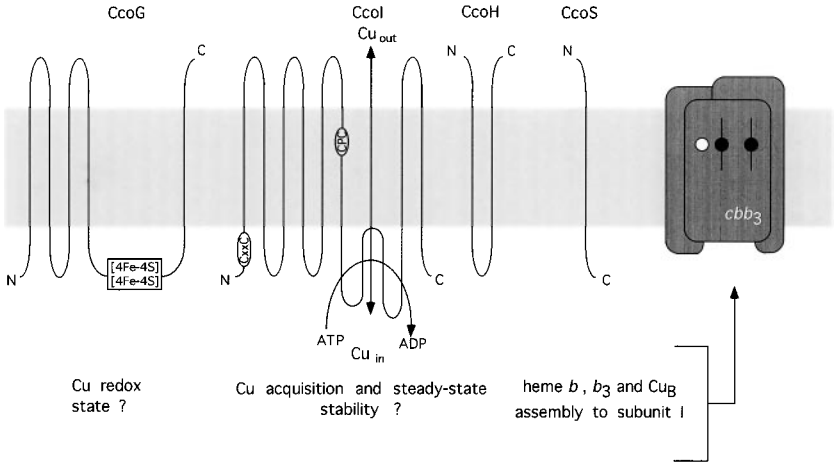

Figure 8. A working model summarizing the roles of *cco*GHIS products in the biogenesis of *R. capsulatus* cyt *cbb*$_3$ oxidase. CcoG may be involved in Cu ion redox state while CcoH and CcoI affect the steady-state amounts of the cyt *cbb*$_3$ oxidase possibly *via* Cu acquisition, and CcoS is required for in the insertion of the *b*-type heme groups and Cu to the subunit I of the cyt *cbb*$_3$ oxidase. Predicted membrane topologies and salient motifs of the *cco*GHIS products are also shown.

putative transmembrane helices is clearly homologous to CPx-type ATPases. Characteristic landmarks of these metal ion transporters, including the phosphatase domain, the phosphorylation site with a conserved aspartyl residue, the ion translocation motif (CPx, with X representing C, S or H), and the cytoplasmic amino terminal metal binding sequences (CxyC) (Solioz & Vulpe, 1996) are also conserved in *R. capsulatus* CcoI. In this case, the CPC motif located in the sixth putative transmembrane helix (often encountered in Cu-transporting ATPases), and a putative topology putting the ATP binding site in the cytoplasm favors Cu import, rather than export, as a function (Figure 8). Such an uptake ability for CcoI is also consistent with its CxyC motif, apparently characteristic of Cu-uptake ATPases such as CopA of *E. hirae* (Solioz & Vulpe, 1996). Usually, Cu-export ATPases, like CopB of *E. hirae* contain a methionine-histidine-rich domain (Odermatt *et al.*, 1993, Solioz *et al.*, 1995) instead of the CxyC motif, while sharing the other characteristic features of CPx-type ATPases. A possible role for CcoI as a Cu-uptake protein is also supported by the observation that the amount of the cyt *cbb*$_3$ oxidase in a wild-type strain significantly decreases under Cu-depleted growth conditions. *Escherichia coli* growth under limited Cu supply also leads to the degradation of cyt *bo* oxidase (Moody *et al.*, 1997). However, the inability to supplement a CcoI$^-$ mutant with exogenous Cu, and the specificity of CcoI for the cyt *cbb*$_3$ oxidase sets it apart from an all-purpose Cu transporter.

Recent NMR-structure of the Menkes-ATPase demonstrated that the CxyC motifs are indeed the interaction sites between the heavy metal and the CPx-ATPases (Gitschier *et al.*, 1998). In addition, involvement of these motifs in sequestering metal ions until delivery to their physiological targets remains plausible. The metal binding site of the Menkes-ATPase shows the same protein fold as MerP, a bacterial mercury sequestering protein (Gitschier *et al.*, 1998; Steele & Opella, 1997). Recent findings that the concentration of free Cu ion in cells is extremely low (less than one atom/cell) (Rae *et al.*, 1999) underline the presence of efficient Cu transport and sequestering proteins such as CcoI.

CcoS is crucial for the production of an active cyt *cbb*$_3$ oxidase. In a CcoS$^-$ mutant, the cyt *cbb*$_3$ oxidase apoenzyme is fully present in the membranes, but has no activity because of the absence of the *b*-type heme groups and Cu cofactors of its subunit I (Figure 8). Remarkably, the *c*-type heme groups of the subunits II and III (cyt c_p and cyt c_o) are still present. These findings indicate that CcoS affects maturation of the subunit I only, and that the subunits II and III of the cyt *cbb*$_3$ oxidase mature independently *via* cyt *c* biogenesis pathways (Kranz *et al.*, 1998). In a CcoS$^-$ mutant, whether the subunits readily detected in the membranes are assembled together to form a physical entity, and if so, whether they contain any other metal ion instead of Cu awaits purification of inactive apo protein cyt *cbb*$_3$ oxidase.

The absence of both of the *b*-type heme groups and the Cu cofactors in a CcoS$^-$ mutant precludes us from distinguishing whether CcoS is required for the insertion of the *b*-type heme groups, or Cu or both. Metal cofactors such as Cu can be coordinated non-enzymatically by appropriate liganding residues of the apoprotein (Merchant & Dreyfuss, 1998). However, this process is often not specific enough for the ligation of only the kind of metal found in the holo-enzyme. Several specific chaperones, NarJ, MelCl and UreE, accomplishing highly specific metal insertion have been reported for nitrate reductase (Blasco *et al.*, 1998), tyrosinase (Chen *et al.*, 1993) and urease (Lee *et al.*, 1993), respectively. Conceivably, CcoS may also function in a similar way for the cyt *cbb*$_3$ oxidase, but the absence of a metal binding site in CcoS argues against a role in metal ligation. It appears that insertion of Cu is less critical in comparison to the heme groups for the assembly of the cyt *c* oxidases. Mutations of the histidine residues liganding Cu often yield mutants that still contain heme *a* or heme *b*. Conversely, elimination of the histidine

ligands coordinating the heme groups often lead to mutants which are unable to assemble properly (Hosler *et al*., 1993; Zufferey *et al*., 1998). This suggests that a primary role of CcoS may be the insertion of the *b*-type heme groups into the cyt cbb_3 oxidases (Figure 8). If this is the case, then it is not surprising that CcoS is not involved in the maturation of the *a*-type heme group containing cyt aa_3 oxidases.

Finally, it is noteworthy that neither Cu-depletion nor mutations in the *cco*GHIS cluster abolish the ability of *R. capsulatus* to grow aerobically. A Q_{ox}^- mutant of *R. capsulatus* does not grow by respiration in Cu-depleted medium, while a C_{ox}^- mutant does. The nature of *R. capsulatus* Q_{ox} is unknown, but these observations suggest that it does not contain Cu, as indicated by the FTIR spectra. The assignment of the Fe-CO band observed at 1971 cm^{-1} in both GK32 (C_{ox}^-) and BK5 ($CcoS^-$) and as a shoulder in M6G (Q_{ox}^-) is unclear. However, it differs from the FTIR spectral features of the nitric oxide reductase of *P. denitrificans*, which exhibits a negative band at 1977 cm^{-1} for the CO adduct of heme *b*, and a positive band at 1963 cm^{-1} for that of the non-heme Fe^{2+} (Hendriks *et al*., 1998). The FTIR spectrum of the cyt *bd*-type Q_{ox} of *E. coli*, which lacks Cu in its binuclear center, shows a negative band at 1984 cm^{-1}, probably indicating binding of CO to heme *d*, and a positive band at 1974 cm^{-1} for heme *b* Fe-CO interaction (Hill *et al*., 1993). The characterization of *R. capsulatus* Q_{ox} is required to define its nature, and assign its FTIR signals unambiguously.

In summary, we have established here for the first time that the different products of *cco*GHIS cluster are required for different maturation steps during biogenesis of the cyt cbb_3 oxidase. In *R. capsulatus*, CcoG is apparently more related to the onset of the photosynthetic gene expression than to the cyt cbb_3 oxidase. On the other hand, both CcoH and CcoI affect the steady-state presence of the cyt cbb_3 oxidase, possibly due to a defect in Cu acquisition, and CcoS is required for the presence of the heme *b*, heme b_3 and Cu cofactors in its subunit I. Ongoing work will further define the properties of these assembly proteins, and their roles during the biogenesis of *R. capsulatus* cyt cbb_3 oxidase.

Materials and Methods

Bacterial strains and growth conditions

The strains and plasmids used are listed in Table 3. *E. coli* strains harboring plasmids were grown in LB medium supplemented with appropriate antibiotics (100 μg/ml ampicilin, 50 μg/ml kanamycin and 12.5 μg/ml tetracycline). *R. capsulatus* strains were grown in Sistrom's minimal medium A (Med A) (Sistrom, 1960) or in enriched medium MPYE (Daldal *et al*., 1986) at 35 °C photoheterotrophically, or chemoheterotrophically under semi-aerobic or aerobic growth conditions in liquid cultures shaken at 150 or 700 rpm, respectively.

Preparation of copper-depleted Med A growth medium

For this purpose, all glasswares were soaked overnight with 0.01 % (w/v) EDTA and rinsed several times with MilliQ-purified (Millipore Inc.) metal-free water. Components of Med A (solution C, trace elements excluding copper, 0.34 M potassium sulfate, 10 % (w/v) ammonium sulfate, 10 % (w/v) sodium succinate, 5 % (v/v) L-glutamic acid, 2 % (v/v) L-aspartic acid, 10 % (w/v) sodium chloride, 1 mM $CuSO_4$ and 100 × vitamins solution) were prepared using metal-free water, and filter-sterilized using a 0.22 μm filter previously rinsed with metal-free water. Appropriate solutions were metal-depleted by using 10 g of Chelex-100 resin per 200 ml of solution to be treated according to the supplier's recommendations (Biorad Inc.), and as described by Domingue *et al*. (1990). Prior to use, the resin was regenerated using two volumes of 1 M HCl (in metal-free water), five volumes of metal-free water, two volumes of 1 M NaOH (in metal-free water) and rinsed with five volumes of metal-free water. For a liter of Med A medium, 5 ml of 10 % ammonium sulfate, 20 ml of 10 % sodium succinate, 2 ml of 5 % L-glutamic acid, 2 ml of 2 % L-aspartic acid and 5 ml of 10 % sodium chloride were mixed and passed through the Chelex-100 column. This mixture was supplemented with 20 ml of solution C, completed to 1 l with metal-free water and autoclaved in pretreated bottles. Immediately prior to growing cells, this solution was supplemented with 20 ml of 0.34 M potassium phosphate, which was metal-depleted separately using a similar Chelex-100 column, and with 10 ml of 100 × vitamins stock per liter. The metal content of the Cu-depleted media was determined by Inductively Coupled Plasma Atomic Emission Spectroscopy (ICP-AES, courtesy of N. Selamoglu). A Cu content of 1570 nM for Med A, less than 315 nM for Cu-depleted Med A, less than 235 nM for MPYE media, and less than 150 nM for other solutions used, were determined.

Molecular genetic techniques

Standard molecular genetics techniques were performed as described by Sambrook *et al*., (1989). The plasmid pCW1 carrying the entire *cco*GHIS cluster and a small portion of *cco*P immediately upstream of it was constructed by subcloning the 5.5 kb *Pvu*II-*Pst*I fragment of pBKIC (H.-G.K. & F.D., unpublished data) into the *Pst*I-*Eco*RI restriction sites of pBSII (Figure 1). The 5.5 kb *Kpn*I-*Sac*I fragment of pCW1 carrying *cco*GHIS was transferred into the appropriate sites of pRK415, yielding pCW3. The plasmid pCW25 carrying both *cco*NOQP and *cco*GHIS was constructed as follows. First, by site directed mutagenesis using Quickchange kit (Stratagene Inc.) with pCW1 as a template and the primers ccoP/*Nhe*I(1) (5′-CAG ATC CGG GCC GTG GCT AGC TAT GTC CAC AGC CTG-3′) and ccoP/*Nhe*I(2) (5′-CAG GCT GTG GAC ATA GCT AGC CAC GGC CCG GAT CTG-3′) a *Nhe*I restriction site was created in *cco*P located 5′ upstream of *cco*G, yielding pCW23. Then, using pOX15 carrying *cco*NOQP (Koch *et al*. 1998) as a template and the mutagenic primers ccoN/*Kpn*I (5′-GCA GCC CGA CGA CGG TAC CGA TCG CGC CGA TCT-3′) and ccoP/*Nhe*I(2) a *Kpn*I restriction site upstream of *cco*N and a silent *Nhe*I site at the 3′ end of *cco*P were constructed. Next the 3.9 kb *Kpn*I-*Nhe*I PCR fragment containing *cco*NOQP was ligated into the *Kpn*I-*Nhe*I sites of pCW23, yielding pCW24. Finally, the resulting 9.4 kb *Kpn*I-*Sac*I fragment carrying *cco*NOQP-*cco*GHIS was

Table 3. Bacterial strains and plasmids used in this study

Strain or plasmid	Genotype	Relevant phenotypes	Source or reference
A. *E. coli*			
HB101	F$^-$, *pro*A2 *hsd*S20 (r_B^- m_B^-)*rec*A13 *ara*14 *lac*Y1 *gal*K2 *rps*L20 *sup*E44 *xyl*-5 *mtl*-1		Sambrook *et al.* (1989)
XL1-Blue	*rec*A1 *end*A1 *gyr*A96 *thi*-1 *hsdr*17 *sup*E44 *rel*A1 *lac* (F′ *pro*AB *lac*I^{q}ΔM15 Tn10 (Tet^r))		Stratagene
B. *R. capsulatus*			
MT1131	crtD121 Rif^r	wild-type	Daldal *et al.* (1986)
Y262		GTA overproducer	Yen *et al.* (1979)
RGK295	Δ(*fnr*L::*kan*)		Zeilstra-Ryalls *et al.* (1997)
GK32	Δ (*cco*NO::*kan*)	Nadi$^-$	Koch *et al.* (1998)
M6G	crtD121 Rif^r, Δ*qox*-260	Nadi$^+$	Daldal, F. (1988)
BK5	*cco*S	Nadi$^-$	Koch *et al.* (1998)
SS33	*cco*I33	Nadi$^-$	Koch *et al.* (1998)
CW1	Δ (*cco*GHIS::*spe*)	Nadi$^-$	This study
CW2	Δ (*cco*I::*spe*)	Nadi$^-$	This study
CW5	Δ (*cco*G::*spe*)	[a]Nadi$^{+/s}$	This study
CW6	*cco*H::*kan*	Nadi$^-$	This study
BK6/CW3	Δ (*cco*S::*kan*)	Nadi$^-$	This study
C. *Plasmids*			
pRK2013		Kan^r, helper	Ditta *et al.* (1985)
pUC4-Kixx		Kan^r	Pharmacia
pHP45Ω		Amp^r , Spec^r	Prentki & Krisch (1984)
pH 45Ω-kan		Amp^r, Kan^r	Fellay *et al.* (1987)
pBSII	pBluescript II (KS+)	Amp^r	Stratagene
pCW1	*cco*GHIS in pBSII	Amp^r	This study
pCW2	Δ*cco*(GHIS::*spe*) in pCW1	Amp^r, Spec^r	This Study
pCW3	*cco*GHIS in pRK415	Tet^r	This study
pCW5	*cco*GH(ΔI)S in pCW1	Amp^r	This Study
pCW6	*cco*GH(I::*spe*)S in pRK415	Amp^r, Spec^r	This Study
pCW7	Δ*cco*(GHIS::*spe*) in pRK415	Tet^r, Spec^r	This study
pCW8	*cco*GH(I::*spe*)S in pRK415	Tet^r, Spec^r	This study
pCW9	*cco*GH(ΔI)S in pRK415	Tet^r	This study
pCW10	pCW1 with *Eco*72 I site in codon 15 of *cco*G	Amp^r	This Study
pCW11	*cco*(ΔG)HIS in pCW1	Amp^r	This Study
pCW12	*cco* Δ(G::spe)HIS in pCW1	Amp^r, Spec^r	This Study
pCW13	*cco*G(ΔH)IS in pCW1	Amp^r	This Study
pCW14	*cco*G(H::*kan*)IS in pCW1	Amp^r, Kan^r	This Study
pCW15	*cco*(ΔG)HIS in pRK415	Tet^r	This study
pCW16	*cco* Δ(G::spe)HIS in pRK415	Tet^r, Spec^r	This study
pCW17	*cco*G(ΔH)IS in pRK415	Tet^r	This study
pCW18	*cco*G(H::*kan*)IS in pRK415	Tet^r, Kan^r	This study
pCW20	pCW1with C12S mutation in *cco*I	Amp^r	This Study
pCW21	pCW3 with C12S mutation in *cco*I	Tet^r	This study
pCW23	derivative of pCW1 with a silent mutation at the 3′end of*cco*P	Amp^r	This study
pCW24	*cco*NOQP, *cco*GHIS in pBSII	Amp^r	This Study
pCW25	*cco*NOQP and *cco*GHIS in pRK415	Tet^r	This study
pRK404		Tet^r	Ditta *et al.* (1985)
pRK415		Tet^r	Ditta *et al.* (1985)
pBK1	*cco*I′S in pRK404	Tet^r	Koch *et al.* (1998)
pBK1E	*cco*I′S in pRK415 lacking *Bam*HI at its multiple cloning site	Tet^r	Koch *et al.* (1998)
pBK1F	*cco*I′(S::*kan*) in pRK404	Tet^r, Kan^r	This study
pOX15	*cco*NOQP in pRK404	Tet^r	Koch *et al.* (1998)
pS33	*cco*G′HIS′ in pRK404	Tet^r	Koch *et al.* (1998)
pXCA601	promoter less *lac*Z	Tet^r	Adams *et al.* (1989)
pXG2	ORF277-*cco*N::*lac*Z in pXCA601	Tet^r	Koch *et al.* (1998)
pXCAG3	*cco*G::*lac*Z in pXCA601	Tet^r	This study
pXCAH1	*cco*H::*lac*Z in pXCA601	Tet^r	This study
pXCAI2	*cco*I::*lac*Z in pXCA601	Tet^r	This study
pXCAS1	*cco*S::*lac*Z in pXCA601	Tet^r	This study

[a] Nadi$^+$ on MedA, Nadi^s on MYPE.

ligated into the appropriate sites of pRK415, yielding pCW25 (Figure 1).

The amino acid residue cysteine 12 of the Cys9-Ala-Val-Cys12 motif of CcoI was replaced with a serine residue *via* site-directed mutagenesis using pCW1 as a template and the primers ccoI12C-S(1) (5′-CCA TTG CGC GGT CTC GAT CAC CGA TGT CG-3′) and its complement ccoI12C-S(2) yielding pCW20. The 5.5 kb *Kpn*I-

*Sac*II fragment of pCW20 was then transferred into the corresponding sites of pRK415, resulting in pCW21.

Construction of various plasmid-borne non-polar *cco*GHIS mutations

For the non-polar in-frame deletion mutation in *cco*G a silent *Eco*72 I restriction site was introduced by site-directed mutagenesis at amino acid position 15 of CcoG using pCW1 as a template and the mutagenic primers MPml1 (5′-GCC GCT TTA TCA CGT GCG TGA ACC GA-3′) and its complement MPml2, yielding pCW10. Digestion of pCW10 with *Eco*72 I and religation deleted approximately 500 bp of *cco*G, yielding pCW11. The 5 kb-long *Kpn*I-*Sac*I fragment of pCW11 carrying a deletion allele of *cco*G was then transferred using the same restriction sites into pRK415, yielding pCW15. A non-polar in-frame deletion of *cco*H was constructed by digesting pCW1 with *Ppu*MI and *Rsr*II, which deleted a 300 bp fragment, yielding pCW13. This deletion allele of *cco*H was then cloned as a 5.2 kb *Kpn*I-*Sac*I fragment into the appropriate sites of pRK415, yielding pCW17. A non-polar deletion of *cco*I was obtained by deleting the 800 bp-long *Sph*I fragment of pCW1 and religation after appropriate treatment, yielding pCW5. The 4.7 kb *Kpn*I-*Sac*I fragment of pCW5 was then cloned into the corresponding sites of pRK415 to yield pCW9.

Construction of various plasmid-borne polar *cco*GHIS mutations and their chromosomal derivatives

To isolate a deletion-insertion allele encompassing *cco*GHIS, the 3.8 kb *Nru*I fragment of pCW1 was replaced by the 2 kb long polar Spe^R cartridge of pHP45Ω (Prentki & Krisch, 1984), yielding pCW2. The Δ(*cco*GHIS::*spe*) allele thus obtained was subcloned into pRK415, yielding pCW7, which was then conjugated into the gene transfer agent (GTA) overproducer strain Y262 of *R. capsulatus* (Yen *et al.*, 1979). The Δ(*cco*GHIS::*spe*) mutation was introduced into the chromosome of MT1131 by homologous recombination *via* GTA cross as described above (Koch *et al.*, 1998), and yielded the mutant CW1 (Figure 2).

The polar deletion-insertion allele Δ(*cco*G::*spe*) was constructed by inserting the same Spe^R cartridge into the *Eco*72 I site of pCW10, yielding pCW12. The *Kpn*I-*Sac*I fragment of pCW12 was cloned into the same sites of pRK415, yielding pCW16. The Δ(*cco*G::*spe*) mutation was introduced into the chromosome of MT1131 as above using GTA, and yielded the mutant CW5 (Figure 2). For constructing a polar *cco*H::*kan* insertion, pCW1 was digested with *Ppu*MI, the 3′ recessive ends thus generated were filled in and ligated to the 2 kb-long polar Kan^R cartridge of pHP45Ω-KM (Fellay *et al.*, 1987), yielding pCW14. The 7.2 kb *Kpn*I-*Sac*I fragment of pCW14 was cloned into pRK415 using the same restriction sites, yielding pCW18. The *cco*H::*kan* allele thus obtained was introduced into the chromosome of MT1131 as above using GTA and yielded the mutant CW6 (Figure 2).

A polar deletion-insertion allele *cco*I::*spe* was constructed by cloning the above described Spe^R cartridge into the appropriately treated *Sph*I site of pCW1, yielding pCW6. The 7.7 kb *Kpn*I-*Sac*I fragment of pCW6 was then subcloned into pRK415, yielding pCW8. The Δ(*cco*I::*spe*) allele thus obtained was introduced into the chromosome of MT1131 *via* a GTA cross and yielded the mutant CW2 (Figure 2). The plasmid pBK1E was constructed by subcloning the 1.3 kb *Hin*dIII-*Stu*I fragment of pBK1 (Figure 1) into a pRK404 derivative lacking the *Bam*HI site at its multiple cloning site. The 0.15 kb *Bam*HI fragment of pBK1E was deleted and replaced with the Kan^R cartridge of pUC4-Kixx, resulting in pBK1F. The Δ(*cco*S::*kan*) deletion-insertion allele was introduced into the chromosome of MT1131 *via* a GTA cross and yielded the mutant BK6 (Figure 2).

Construction of *cco*G::*lacZ*, *cco*H::*lacZ*, *cco*I::*lacZ* and *cco*S::*lacZ* fusion

All fusions were constructed by using PCR with 50 to 150 ng of pCW1 as a template, 0.5 mM of each deoxynucleoside triphosphate, 125 ng of each primer, 15% (v/v) glycerol, 2.5 units of *Pfu* polymerase. The reaction mixtures were incubated at 98 °C for 30 seconds prior to the first cycle, followed by 30 cycles of (97 °C for 30 seconds, 60 °C for 20 seconds, and 72 ° C for 110 seconds). For the *cco*G::*lacZ* translational fusion carried by pXCAG3, the 5′ upstream region of *cco*G was amplified using the primers PstIccoGgal (5′-GCC GTC CTG CAG CTG GGC GGC CGA TGG CGC GAA-3′) and *Bam*HIccoGgal (5′-ACT TGG TGG ATC CGC GCT CAT GGG TGT CTC CGT-3′), resulting in a 280 bp fragment encompassing the first three codons of *cco*G. For the *cco*H::*lacZ* translational fusion carried by pXCAH1 the 5′ upstream region of *cco*H was amplified using *Pst*IccoHgal (5′-CGC ACG CTG GAG TAT TTC ACG CTC TGG TCG GGC-3′) and *Bam*HIccoHgal (5′-CAT CAG CGG ATC CTT GCG GCC GGT CAG CGG TTT-3′) primers, yielding a 460 bp fragment encompassing the first nine codons of *cco*H. For the *cco*I::*lacZ* translational fusion carried by pXCAI2, the 5′ upstream 580 bp region of *cco*I including its first three codons was amplified by using the primers *Pst*IccoIgal (5′-AAG GTC CTG CAG ATG TTC GTG GCC TTC TTC GGG-3′) and *Bam*HIccoIgal (5′-GGC GGT GGG ATC CGA GAG CAT GAT CCG CGC CCC-3′). For the *cco*S::*lacZ* translational fusion carried by pXCAS1, the 454 bp 5′ upstream region of *cco*S including its first seven codons were amplified by using the primers *Pst*IccoSgal (5′-TCG GCG CTG CAG GGC AAG CTT GCA TCA CCG AAT-3′) and *Bam*HIccoSgal (5′-CGA GAT CGG ATC CAG ATA GGT CAG GAC CGA CAT-3′). The PCR products thus obtained were digested with *Bam*HI and *Pst*I restriction enzymes, except for *cco*G::*lacZ* where only *Bam*HI was used, and cloned into the corresponding sites of the conjugative promoter-probe vector pXCA601 (Adams *et al.*, 1989), which contains an in-frame *Bam*HI site at the 5′ end of *lacZ*. The junction regions of the plasmids pXCAG3, pXCAH1, pXCAI2 and pXCAS1 were sequenced as described below to confirm that they carried in-frame translational *lacZ* fusions.

DNA sequence analyses

Automated DNA sequencing with a dye terminator cycle sequencing kit (Amplitaq FS, Applied Biosystems) was used as specified by the manufacturer. Appropriate derivatives of pCW1 and pRK415 were used as double stranded DNA templates and the following primers (5′ to 3′ orientation) synthesized at the DNA Synthesis Service, Department of Chemistry, University of Pennsylvania or ordered from Gibco-BRL, as sequencing primers: CCOP7271, GCAATATAGCTTTAAGGTGC; CCOG8721, AAGCGCACCGAGATCATGAT; CI4, AACAGCTTGCC CGACGCC; BK1, TAGCCCGAACGGAGCCCAAG; MG 1E, ATGCGAAGACGATCACCACC; seqI9340, CGCTT

CCGCCTGCCCGGCCT; COS-1, TTCGTGATCTCCGCC GCCTATAAC; and COS-2, GTCGATTGTTCGGTGA TCG. The nucleotide sequence of the *cco*S alleles in mutants BK5 and BK6 was determined using PCR products obtained with the mutant chromosomal DNA as templates and COS-1 and COS-2 as sequencing primers.

DNA analysis, predictions for segmental flexibility in amino acid sequences, and homology searches were done using MacVector (IBI, Kodak) and BLAST programs (Altschul *et al*., 1990). The computer program TmPred (Hoffmann & Stoffel, 1993) and Clustal W (Thompson *et al*., 1994) were used to predict the possible transmembrane helices and for sequence alignments, respectively.

Isolation of chromatophore membranes, immunoblots and heme staining

R. capsulatus intracytoplasmic membrane vesicles (chromatophores) were prepared in 20 mM Mops (3-(*N*-morpholino)propanesulfonic acid) (pH 7.0) containing 1 mM KCl and 0.4 mM Pefabloc SC (Boehringer Mannheim, Germany) by using a French pressure cell as described by Gray *et al*. (1994). They were analyzed using a 16.5 % or 10 % sodium dodecyl sulfate-polyacrylamide gel electrophoresis, according to Schägger and von Jagow (1987). Samples were solubilized in 3 % SDS and 5 % β-mercaptoethanol and incubated for 15 minutes at 75 °C. Cytochromes containing *c*-type heme groups were revealed by treating the gel with 3,3′,5,5′-tetramethylbenzidine (TMBZ) according to Thomas *et al*. (1976). For immunoblot analysis, proteins were electroblotted onto Immobilon-P membranes, and polyclonal antibodies prepared against *R. capsulatus* CcoP and CcoN (Koch *et al*., 1998) and purified by using thiophilic adsorption chromatography (Pierce, Rockford USA) according to the manufacturer's specifications were used. Horseradish peroxidase-conjugated goat anti-rabbit antibodies (Bio-Rad, Richmond, CA) were used as secondary antibodies, with diaminobenzidine as a peroxidase substrate enhanced with $NiCl_2$.

Enzyme assays

C_{ox} positive colonies were detected by staining the plates with a 1:1 (v/v) mixture of 35 mM α-naphthol dissolved in ethanol and 30 mM *N,N*-dimethyl-*p*-phenylene diamine in water (Keilin, 1966). Under these conditions, colonies that exhibit C_{ox} activity turn blue within 30 seconds ($Nadi^+$ phenotype). Ascorbate/2,3,5,6-tetramethyl-1,4-phenylenediamine (TMPD) oxidase activity was measured polarographically using a Clark-type oxygen electrode (YSI Inc., Yellow Springs, OH) and chromatophore membranes at a protein concentration of about 0.1 mg/ml in 50 mM Mops buffer, pH 7.0, and 5 mM $MgCl_2$. Oxygen consumption, initiated by the addition of 10 mM sodium-ascorbate and 200 μM TMPD, and subsequently inhibited by 100 μM KCN, was recorded. Net TMPD oxidase activity was determined by subtracting the cyanide insensitive respiratory rate from that induced by ascorbate. For β-galactosidase activity assays cultures were grown as appropriate, cells were harvested at an A_{630} of 0.4 to 0.6 nm, washed with water, and resuspended in 1 ml of Z-buffer (60 mM Na_2HPO_4, $7H_2O$, 40 mM NaH_2PO_4 H_2O, 10 mM KCl, 1 mM $MgSO_4$ $7H_2O$ and 50 mM β-mercaptoethanol, pH 7.0) and disrupted by sonication. The β-galactosidase activity (in duplicate) was determined using 5 to 30 μl of crude extracts added to 1 ml of Z-buffer and 200 μl of *o*-nitrophenyl-β-D-galactopyranoside (ONPG) (4 mg/ml) at 35 °C for five to 15 minutes (Miller, 1972). The linearity of the assay was checked using various amounts of extracts incubated for various length of time. The reaction was stopped by addition of 0.5 ml of 1 M sodium carbonate, absorbance at 420 nm was recorded and an ε_{ONPG} of 21300 M^{-1} cm^{-1} was used. Units of activity refer to nmoles of ONPG hydrolyzed per minute per ml and per mg of proteins. Protein concentrations were determined according to Lowry *et al*., (1951).

Spectroscopic techniques

Anaerobic, dark reductive potentiometric titrations of chromatophore membranes were performed according to Dutton (1978) as described by Gray *et al*. (1994), monitoring absorbance differences at 550 *minus* 540 nm for cyt *c* and 560 minus 570 nm for cyt *b*, respectively.

For Fourrier-transformed infrared (FTIR) spectroscopy cells were grown semiaerobically in MPYE medium, and chromatophore membranes prepared as described above, except that membranes were washed and resuspended in 50 mM Tris (pH 7.5) to a final protein concentration of 40 mg/ml. For preparation of CO adducts 3 ml of membranes were transferred to a Ti60 ultracentrifugation tube sealed with a rubber septum, and made anaerobic by repeated cycles of vacuum and argon flushing. Anaerobically prepared Na-ascorbate and TMPD were added to a final concentration of 10 mM and 200 μM, respectively, and membranes were incubated for 30 minutes at room temperature. CO was added to the reduced anaerobic membranes by repeated cycles of vacuum and CO flushing, and samples were incubated for at least 180 minutes at 48 °C. Membranes were then pelleted at 160,000 *g* for 90 minutes and the supernatant was decanted under a flow of CO. The pellet was overlaid with CO-saturated glycerol to dehydrate the sample, and extracted for at least 12 hours at 4 °C. A portion of the dehydrated sample was pressed between two CaF_2 windows and mounted into a cryostat. Infrared spectra were obtained with a Matteson Sirius 100 FTIR interferometer at a resolution of 0.5 cm^{-1}. A liquid nitrogen-cooled indium antimonide detector was used to observe the spectra in the 1750-3000 cm^{-1} range. Interferograms were detected in a single-beam mode and an average of 512 scans were recorded. Spectra are presented as difference spectra obtained by subtracting the spectrum taken before photolysis (dark) from that taken after photolysis (light). Photodissociation was achieved by using a focused 500 W tungsten bulb, and heat and UV radiation were minimized by passage through water and glass.

Chemicals

Unless otherwise noted all chemicals were of reagent grade and obtained from commercial sources.

Acknowledgments

This work was supported by grants from NIH GM 38237 to F.D. We thank O. Hwang for her help with initial screening of the Nadi-minus mutants.

References

Adams, C. W., Forrest, M. E., Cohen, S. N. & Beatty, J. T. (1989). Structural and functional analysis of transcriptional control of the *Rhodobacter capsulatus puf* operon. *J. Bacteriol.* **171**, 473-482.

Alben, J. O. (1993). Analysis of relaxation processes helps to define molecular states in biological systems. *Biophys. J.* **65**, 1357-1358.

Altschul, S. F., Gish, W., Miller, W., Myers, E. W. & Lipman, D. J. (1990). Basic local alignment search tool. *J. Mol. Biol.* **215**, 403-410.

Batut, J. & Boistard, P. (1994). Oxygen control in *Rhizobium*. *Antonie van Leeuwenhoek,* **66**, 129-150.

Beinert, H., Holm, R. H. & Munck, E. (1997). Iron-sulfur clusters: nature's modular, multipurpose structures. *Science,* **277**, 653-659.

Blasco, F., Dos, Santos J. P., Magalon, A., Frixon, C., Guigliarelli, B., Santini, C. L. & Giordano, G. (1998). NarJ is a specific chaperone required for molybdenum cofactor assembly in nitrate reductase A of *Escherichia coli*. *Mol. Microbiol.* **28**, 435-447.

Chen, L. Y., Chen, M. Y., Leu, W. M., Tsai, T. Y. & Lee, Y. H. (1993). Mutational study of *Streptomyces* tyrosinase trans-activator MelC1. MelC1 is likely a chaperone for apotyrosinase. *J. Biol. Chem.* **268**, 18710-18716.

Daldal, F. (1988). Cytochrome c_2-independent respiratory growth of *Rhodobacter capsulatas*. *J. Bacteriol.* **170**, 2388-2391.

Daldal, F., Cheng, S., Applebaum, J., Davidson, E. & Prince, R. C. (1986). *Cyt*ochrome c_2 is not essential for photosynthetic growth of *Rhodopseudomonas capsulata*. *Proc. Natl Acad. Sci. USA,* **83**, 2012-2016.

Ditta, G., Schmidhauser, T., Yacobson, E., Lu, P., Liang, X.-W., Finlay, D. R., Guiney, D. & Helsinki, D. R. (1985). Plasmids related to the broad host range vector, pRK290, useful for gene cloning and for monitoring gene expression. *Plasmid,* **13**, 149-153.

Domingue, P. A. G., Mottle, B., Morck, D. W., Brown, M. R. W. & Costerton, J. W. (1990). A simple rapid method for the removal of iron and other cations from complex media. *J. Microbiol. Methods,* **12**, 13-22.

Dutton, P. L. (1978). Redox potentiometry: determination of midpoint potentials of oxidation-reduction components of biological electron transfer systems. *Methods Enzymol.* **54**, 411-435.

Fellay, R., Frey, J. & Krisch, H. (1987). Interposon mutagenesis of soil and water bacteria: a family of DNA fragments designed for *in vitro* insertional mutagenesis of Gram-negative bacteria. *Gene,* **52**, 147-154.

Fiamingo, F. G. & Alben, J. O. (1985). Structures of photolyzed carboxymyoglobin. *Biochemistry,* **24**, 7964-7970.

Fiamingo, F. G., Altschuld, R. A., Moh, P. P. & Alben, J. O. (1982). Dynamic interactions of CO with a_3Fe and Cu_B in cytochrome *c* oxidase in beef heart mitochondria studied by Fourier transform infrared spectroscopy at low temperatures. *J. Biol. Chem.* **257**, 1639-1650.

Garcia-Horsman, A., Berry, E., Shapleigh, J. P., Alben, J. O. & Gennis, R. B. (1994a). A novel cytochrome *c* oxidase from *Rhodobacter sphaeroides* that lacks Cu_A. *Biochemistry,* **33**, 3113-3119.

Garcia-Horsman, J. A., Barquera, B., Rumbley, J., Ma, J. & Gennis, R. B. (1994b). The superfamily of heme-copper respiratory oxidases. *J. Bacteriol.* **176**, 5587-5600.

de Gier, J.-W., Schepper, M., Reijnders, W. N. M., van Dyck, S. J., Slotboom, D. J., Warne, A., Saraste, M., Kraab, K., Finel, M., Stouthamer, A. H., van Spanning, R. J. M. & van der Oost, J. (1996). Structural and functional analysis of aa_3-type and cbb_3-type cytochrome *c* oxidase of *Paracoccus denitrificans* reveals significant differences in proton-pump design. *Mol. Microbiol.* **20**, 1247-1260.

Gitschier, J., Moffat, B., Reilly, D., Wood, W. I. & Fairbrother, W. J. (1998). Solution structure of the fourth metal-binding domain from the Menkes copper-transporting ATPase. *Nature Struct. Biol.* **5**, 47-54.

Gray, K. A., Grooms, M., Myllykallio, H., Moomaw, C., Slaughter, C. & Daldal, F. (1994). *Rhodobacter capsulatus* contains a novel *cb*-type cytochrome *c* oxidase without a Cu_A center. *Biochemistry,* **33**, 3120-3127.

Hassett, R. & Kosman, D. J. (1995). Evidence for Cu(II) reduction as a component of copper uptake by *Saccharomyces cerevisiae*. *J. Biol. Chem.* **270**, 128-134.

Hendriks, J., Warne, A., Gohlke, U., Haltia, T., Ludovici, C., Lübben, M. & Saraste, M. (1998). The active site of the bacterial nitric oxide reductase is a dinuclear iron center. *Biochemistry,* **37**, 13102-13109.

Hill, J. J., Alben, J. O. & Gennis, R. B. (1993). Spectroscopic evidence for a heme-heme binuclear center in the cytochrome *bd* ubiquinol oxidase from *Escherichia coli*. *Proc. Natl Acad. Sci. USA,* **90**, 5863-5867.

Hoffmann, K. & Stoffel, W. (1993). TMbase-a database of membrane spanning protein segments. *J. Biol. Chem.* **268**, 166.

Hosler, J. P., Ferguson-Miller, S., Calhoun, M. W., Thomas, J. W., Hill, J., Lemieux, L., Ma, J., Georgiou, C., Fetter, J., Shapleight, J., Tecklenburg, M. J., Babcock, G. T. & Gennis, R. B. (1993). Insight into the active site structure and function of cytochrome oxidase by analysis of site-directed mutants of bacterial cytochrome aa_3 and cytochrome *bo*. *J. Bioenerg. Biomembr.* **25**, 121-136.

Kahn, D., David, M., Domergue, O., Daveran, M.-L., Ghai, J., Hirsch, P. R., . & Batut, J. (1989). *Rhizobium meliloti fixGHI* sequence predicts involvement of a specific cation pump in symbiotic nitrogen fixation. *J. Bacteriol.* **171**, 929-939.

Keilin, D. (1966). *The History of Cell Respiration and Cytochrome*, Cambridge University Press, Cambridge, UK.

Koch, H.-G., Hwang, O. & Daldal, F. (1998). Isolation and characterization of *Rhodobacter capsulatus* mutants affected in cytochrome cbb_3 oxidase activity. *J. Bacteriol.* **180**, 969-978.

Kranz, R., Lill, R., Goldman, B., Bonnard, G. & Merchant, S. (1998). Molecular mechanisms of cytochrome *c* biogenesis: three distinct systems. *Mol. Microbiol.* **29**, 383-396.

La Monica, R. F. & Marrs, B. L. (1976). The branched respiratory system of photosynthetically grown *Rhodopseudomonas capsulata*. *Biochim. Biophys. Acta,* **423**, 431-439.

Lee, M. H., Pankratz, H. S., Wang, S., Scott, R. A., Finnegan, M. G., Johnson, M. K., Ippolito, J. A., Christianson, D. W. & Hausinger, R. P. (1993). Purification and characterization of *Klebsiella aerogenes* UreE protein: a nickel-binding protein that functions in urease metallocenter assembly. *Protein Sci.* **2**, 1042-1052.

Lowry, O., Rosebrough, N., Farr, A. & Randall, R. (1951). Protein measurement with the Folin phenol reagent. *J. Biol. Chem.* **193**, 265-275.

Lutsenko, S., Petrukhin, K., Cooper, M. J., Gillian, C. T. & Kaplan, J. H. (1997). N-terminal domains of human copper-transporting adenosine triphosphatase (the Wilson's and Menkes disease proteins) bind copper selectively *in vivo* and *in vitro* with stoichiometry of one copper per metal-binding repeat. *J. Biol. Chem.* **272**, 18939-18944.

Merchant, S. & Dreyfuss, B. W. (1998). Posttranslational assembly of photosynthetic metalloproteins. *Annu. Rev. Plant Physiol. Plant Mol. Biol.* **49**, 25-51.

Miller, J. H. (1972). *Experiments in Molecular Genetics*, Cold Spring Harbor Laboratory Press, Cold Spring Harbor, NY.

Moody, A. J., Mitchel, R., Jeal, A. E. & Rich, P. R. (1997). Comparison of the ligand-binding properties of native and copper-less cytochromes *bo* from *Escherichia coli*. *Biochem. J.* **324**, 743-752.

Mouncey, N. J. & Kaplan, S. (1998). Oxygen regulation of the *cco*N gene encoding a component of the ccb_3 oxidase in *Rhodobacter sphaeroides* $2.4.1^T$: Involvement of the FnrL Protein. *J. Bacteriol.* **180**, 2228-2231.

Neidle, E. L. & Kaplan, S. (1992)). Rhodobacter sphaeroides rdxA, a homolog of *Rhizobium meliloti fix*G, encodes a membrane protein which may bind cytoplasmic (4Fe-4S) clusters. *J. Bacteriol.* **174**, 6444-6454.

Odermatt, A., Suter, H., Krapf, R. & Solioz, M. (1993). Primary structure of two P-type ATPases involved in Copper homeostasis in *Enterococcus hirae*. *J. Biol. Chem.* **268**, 12775-12779.

O'Gara, J. P. & Kaplan, S. (1997). Evidence for the role of redox carriers in photosynthesis gene expression and carotenoid biosynthesis in *Rhodobacter sphaeroides* 2.4.1. *J. Bacteriol.* **179**, 1951-1961.

Oh, J., II & Kaplan, S. (1999). The cbb_3 terminal oxidase of *Rhodobacter sphaeroides* 2.4.1: Structural and functional implications for the regulation of spectral complex formation. *Biochemistry,* **38**, 2688-2696.

Preisig, O., Zufferey, R. & Hennecke, H. (1996). The *Bradyrhizobium japonicum fixGHIS* genes are required for the formation of the high-affinity cbb_3-type cytochrome oxidase. *Arch. Microbiol.* **165**, 297-305.

Preisig, O., Anthamatten, D. & Hennecke, H. (1993). Genes for a microaerobically induced oxidase complex in *Bradyrhizobium japonicum* are essential for a nitrogen-fixing endosymbiosis. *Biochemistry,* **90**, 3309-3313.

Prentki, P. & Krisch, H. M. (1984). *In vitro* insertional mutagenesis with a selectable DNA fragment. *Gene,* **29**, 303-313.

Rae, T. D., Schmidt, P. J., Pufahl, R. A., Culotta, V. C. & O'Halloran, T. V. (1999). Undetectable intracellular free copper: The requirement of a copper chaperone for superoxide dismutase. *Science,* **284**, 805-808.

Sambrook, J., Fritsch, E. F. & Maniatis, T. (1989). *Molecular Cloning: A Laboratory Manual*, Cold Spring Harbor Laboratory Press, Cold Spring Harbor, NY.

Schägger, H. & von Jagow, G. (1987). Tricine-sodium dodecyl sulfate polyacrylamide gel electrophoresis for the separation of proteins in the range from 1 to 100 kDa. *Anal. Biochem.* **166**, 368-379.

Sistrom, W. (1960). A requirement for sodium in the growth of *Rhodopseudomonas sphaeroides*. *J. Gen. Microbiol.* **22**, 778-785.

Solioz, M. & Vulpe, C. (1996). CPx-type ATPases: a class of P-type ATPases that pump heavy metals. *Trends Biochem. Sci.* **21**, 237-241.

Solioz, M. & Odermatt, A. (1995). Copper and silver transport by CopB-ATPase in membrane vesicles of *Enterococcus hirae*. *J. Biol. Chem.* **270**, 9217-9221.

Steele, R. A. & Opella, S. J. (1997). Structures of the reduced and mercury-bound forms of MerP, the periplasmic protein from the bacterial mercury detoxification system. *Biochemistry,* **36**, 6885-6895.

Thöny-Meyer, L., Beck, C., Preisig, O. & Hennecke, H. (1994). The *ccoNOQP* gene cluster codes for a *cb*-type *cyt*ochrome oxidase that functions in aerobic respiration of *Rhodobacter capsulatus*. *Mol. Microbiol.* **174**, 705-716.

Thomas, P. E., Ryan, H. & Levin, H. (1976). An improved staining procedure for the detection of the peroxidase activity of cytochrome P-450 on sodium dodecyl sulfate polyacrylamide gels. *Anal. Biochem.* **75**, 168-176.

Thompson, J., Higgins, D. & Gibson, T. (1994). CLUSTAL W: improving the sensitivity of progressive multiple sequence alignment through sequence weighting, position-specific gap penalties and weight matrix choice. *Nucl. Acids Res.* **22**, 4673-4680.

Vulpe, C., Levinson, B., Whitney, S., Packman, S. & Gitschier, J. (1993). Isolation of a candidate gene for Menkes disease and evidence that it encodes a copper transporting ATPase. *Nature Genet.* **3**, 7-13.

Yen, H. C., Hu, N. T. & Marrs, B. L. (1979). Characterization of the gene transfer agent made by an overproducer mutant of *Rhodopseudomonas capsulata*. *J. Mol. Biol.* **131**, 157-168.

Zannoni, D. (1995). Aerobic and anaerobic electron transport chains in anoxygenic phototrophic bacteria. In *Anoxygenic Photosynthetic Bacteria* (Blankenship, R. E., Madigan, M. T. & Bauer, C. E., eds), pp. 949-971, Kluwer Academic Publishers, Dordrecht, Netherlands.

Zannoni, D., Melandri, B. & Baccarini-Melandri, A. (1976). Energy transduction in photosynthetic bacteria: Composition and function of the branched oxidase system in wild-type and respiration deficient mutants of *Rhodopseudomonas capsulata*. *Biochim. Biophys. Acta,* **423**, 413-430.

Zeilstra-Ryalls, J. H., Gabbert, K., Mouncey, N. J., Kaplan, S. & Kranz, R. G. (1997). Analysis of the *fnr*L gene and its function in *Rhodobacter capsulatus*. *J. Bacteriol.* **179**, 7264-7273.

Zufferey, R., Engin, A., Thöny-Meyer, L. & Hennecke, H. (1998). How replacements of the 12 conserved histidines of subunit I affects assembly, cofactor binding, and enzymatic activity of *Bradyrhizobium japonicum* cbb_3 oxidase. *J. Biol. Chem.* **273**, 6452-6459.

Edited by M. Gottesman

(Received 14 October 1999; received in revised form 10 January 2000; accepted 20 January 2000)